Active debris removal using electromagnetic induction

I.K. Patel[1], V.S. Aslanov[1]

[1]Samara National Research University, Moskovskoe Shosse 34A, Samara, Russia, 443086

Abstract. The present study discusses the technique for active space debris removal using electromagnetically induced force in electrically conductive materials. The force in action is called Lorentz force which acts on an electrically conductive material when it is moving through uniform or non-uniform magnetic field distribution. The basic principle of this idea is in accordance to Faraday's law of induction and Lenz's law. In this paper, focus is on developing a method to capture or accelerate/decelerate the electrically conductive debris with the goal of transferring it to a separate orbit such as, graveyard orbit. For the current idea, a hypothetical toroidal coil is assumed to generate sufficiently strong magnetic field when applied electrical current, which is realized on the debris in motion. Orbital dynamics of the debris is studied incorporating the proposed method and results are drawn. The applicability of the idea is discussed and, areas of improvement and further study are recognized.

1. Introduction

The number of space debris objects have greatly increased over the past few decades. According to the latest report generated by the Astronomical Research and Exploration Science (ARES) for the population of space debris objects in the orbital environment of Earth, there are approximately 500,000 objects having diameter – 1 cm to 10 cm [1]. Objects larger than 10 cm are estimated to be more than 23,000 and objects smaller than 1 mm exceeds the count – 100 million [1]. Considerable effort is put into detecting the space debris using ground-based instruments and generating evolution models for the debris population [2]. In the near future, active debris removal will become necessary to mitigate the risk of hazardous collisions [3].

In general, active debris removal techniques are divided into two groups: contact and contactless debris removal. Contact debris removal techniques employ a contact medium such as robotic arm or tether to attach to the target object. This technique is rather complicated in application of capturing tumbling objects using rigid contact medium due to its limited degrees of freedom. For example, the largest rotational speed that can be tolerated by a rigid medium is 4–5 degrees per second [4]. Contactless techniques have a major advantage over contact techniques because intricacies related to capturing and holding an object in accelerating motion are avoided [5, 6]. However, current contactless techniques provide no control over the resulting trajectory of the captured object after it leaves the control satellite.

Accounting for the limitations of the current debris removal techniques, a new method is developed, which can be applied to safely capture or change the trajectory of the debris object in a controllable manner. The present study is focused on the application of a torus-shaped magnetic field generator to collect or transfer the target object into a different orbit. The proposed system works on the basis of Lorentz force and Faraday's law of induction.

2. Magnetic force analysis

2.1 Fundamentals and Theory

Earth's magnetic field is one of the fundamental perturbative forces that significantly affects the motion of objects in near earth orbit (NEO). The strength of the magnetic perturbation decreases with higher altitude, such that the effects of Earth's magnetic field are considerably low to be neglected at altitude of geosynchronous orbit and higher [7]. Observations show that Earth's magnetic field generates angular torques on the rotating objects in orbit which tends to slow down its rotational motion. This effect is attributable to the induction of magnetic field in a conducting object when it is moving through magnetic field. The effect is described by *Lenz's law*. The induced magnetic field generates eddy currents flowing in closed loops with the direction determined by the direction of magnetic field acting on the object and motion of the object itself. Additionally, if the object is moving through a non-uniform magnetic field, a well-known force appears to work on the object, called Lorentz force.

In order to develop a useful technique for contactless debris removal it is required to present the fundamental laws that govern the characteristics of magnetic interaction of the space debris.

The discovery of electromagnetism by Faraday in 1830 was a monumental event in the history of science. He experimented with the setup of moving metallic coil between magnetic poles. He discovered that the electric current is induced in the coil subject to motion of the coil though the magnetic field. Later the phenomenon came to be known as generation of *eddy currents* due to time-varying magnetic field [8]. On the basis of the observations made from his experiment he postulated following statements:

- An electromotive force (*e.m.f.*) is induced subject to the change in magnetic flux through the circuit;
- Magnitude of the induced e.m.f. is proportional to the change in magnetic flux.

Moreover, according to *Lenz's law* (1), the direction of induced e.m.f. ε is such that the induced currents opposes the change in magnetic flux φ [9],

$$\varepsilon = -\frac{d\varphi}{dt} = -\frac{\partial}{\partial t}\iint \vec{B}d\vec{S} = \oint \vec{E}d\vec{l} \tag{1}$$

Where $\vec{B}$ is the external magnetic field vector and S is the surface generic to electric coil.

An important consequence of equation (1) is Maxwell's third equation as the generalisation of Faraday's law, which can be derived by applying *Stoke's law* (2) as following,

$$\nabla \times \vec{E} = -\frac{\partial \vec{B}}{\partial t} \tag{2}$$

Equation (2) is valid for any case of changing magnetic flux, the time-variation in magnetic field itself or the motion of the conducting circuit through magnetic field.

Additional field equations related to the laws of electromagnetism are written in the form of four Maxwell's field equations [9],

$$\nabla \cdot \vec{E} = \frac{\rho}{\epsilon_0} \tag{3}$$

$$\nabla \cdot \vec{B} = 0 \tag{4}$$

$$\nabla \times \frac{\vec{B}}{\mu_0} = \vec{j} + \epsilon_0 \frac{\partial \vec{E}}{\partial t} \tag{5}$$

Where ρ is the charge density of the circuit and $\vec{j}$ is current density vector. $\epsilon_0 = 8.854 \cdot 10^{-12}\ F/m$ is the permittivity of vacuum, and $\mu_0 = 4\pi \cdot 10^{-12}\ N/A^2$.

Equation (3) is the mathematical representation of Gauss's law, which states that the total electric field flux through a closed surface is proportional to the ration of material charge density and permittivity of vacuum. Equation (4) is the Gauss's law for magnetism, which states that the total magnetic field flux through a closed surface is zero. Equation (5) is known as *Ampère-Maxwell equation* for electromagnetism, which associates the change in electric field with the induction of circulating magnetic field [9].

An important addition to the Maxwell's equations (4) – (5) is the equation for *Lorentz force*, which corresponds to the force acting on any arbitrary charge particle q or a group of charge particles moving with velocity $\vec{v}$ through an external magnetic field $\vec{B}$ and electric field $\vec{E}$. The formula for Lorentz force is given as following:

$$\vec{F} = q\left(\vec{E} + \vec{v} \times \vec{B}\right) \tag{6}$$

2.2 Lorentz force on a sphere

Assume a spherical debris of radius *a* moving with velocity *v* through non-uniform magnetic field *B* as shown in Figure 1. The inertial reference system at the instant of analysis is fixed in space at the centre *O* of torus with radius *R*.

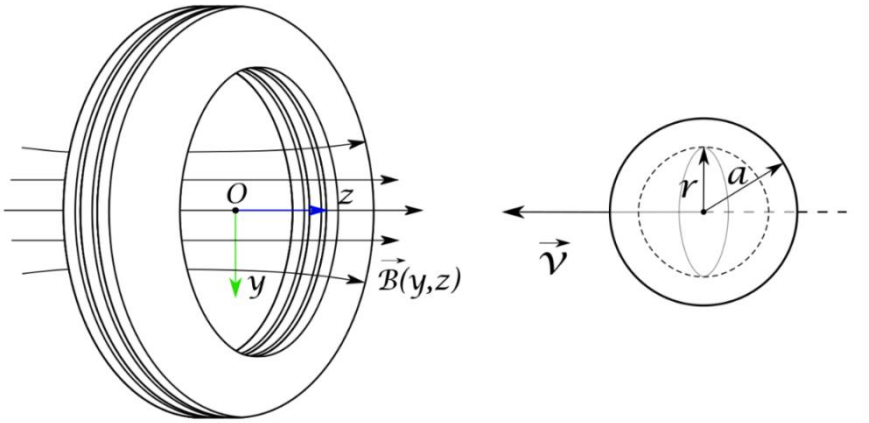

Figure 1. Spherical debris moving through non-uniform magnetic field.

Magnetic field lines close to z-axis are pointed along positive z-axis and varies in strength along y-axis, $B_z(y)$. Expanding the vertical magnetic field vector about point $y = 0$ in the form of Taylor's series, $B_y(z)$ can be written as follows:

$$B_y(z) = B_y(0) + z\frac{\partial B_y(0)}{\partial z} + \frac{z^2}{2}\frac{\partial^2 B_y(0)}{\partial z^2} + \cdots \tag{7}$$

If the peak magnetic field gradient $B_0/2R$ is greater than the radius of the sphere, then higher order terms in expression (7) are considerably smaller than first two terms [10]. Therefore, terms of the order $O(3)$ and higher can be neglected and expression (7) can be rewritten as following:

$$B_y(z) = B_y(0) + z\frac{\partial B_y(0)}{\partial z} \tag{8}$$

Where $B_y(0)$ is constant for a steady magnetic field distribution. Thus, $B_y(0)$ can be replaced in equation (8) with B_0.

Equations (4)-(6) are rewritten for the current problem of motion of the sphere as following:

$$\left.\begin{aligned} \vec{j} \times \vec{B} &= 0 \\ \nabla \cdot \vec{v} &= 0 \\ \nabla \cdot \vec{j} &= 0 \\ \vec{j} &= \sigma\left(-\nabla\phi + \vec{v} \times \vec{B}\right) \end{aligned}\right\} \tag{9}$$

Here $\vec{j}$, σ, $\vec{v}$ and ϕ are induced electric current density, electrical conductivity of sphere, velocity of sphere and potential gradient, respectively.

Velocity of the sphere is directed along negative *z* direction, while magnetic field vector is in the direction as shown in Figure 2. Magnetic field vector $\vec{B}(y,z)$ can be divided into two components: Transverse component B_z and vertical component B_y. Ampère's law implies that the magnetic field is solenoidal for $R \ll 1$, thus it can be assumed that the magnetic field distribution is planar [9]. Consequently, it can be stated that magnetic field does not change along *x* direction and hence following expression can be written.

$$\frac{\partial B_y}{\partial z} = \frac{\partial B_z}{\partial y} \tag{10}$$

From equation (8), it follows that $\partial B_z/\partial y \neq 0$ implying that $B_y \neq 0$.

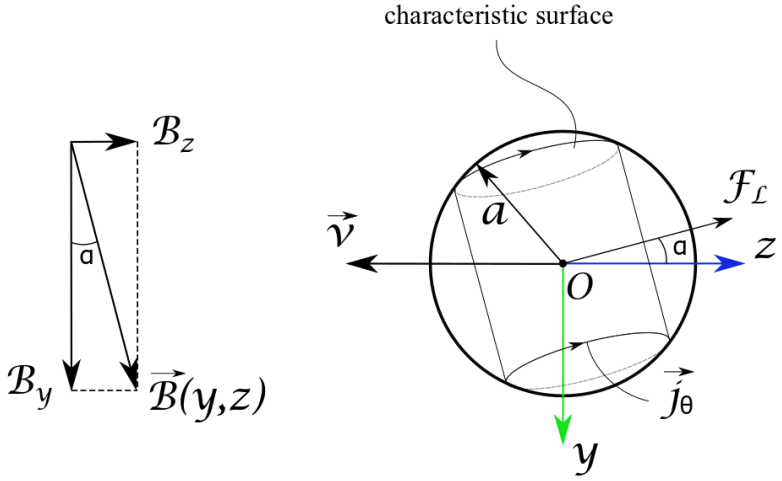

Figure 2. Effect of non-uniform magnetic field on the motion of sphere.

Pertaining to non-uniformity of the magnetic field lines, eddy currents flow around the cylindrical characteristic surface concentric with the diameter parallel to magnetic field vector $\vec{B}(y,z)$. Direction of electrical current density vector $\vec{j}_\theta$ is determined using Lenz's law. Lorentz force $\vec{F}_L$ always acts in a direction perpendicular to the characteristic surface. Velocity of the sphere can be written in cylindrical coordinate system as, $v\hat{k} = -v\sin\theta\,\hat{e}_r - v\cos\theta\,\hat{e}_\theta$.

To simplify the derivation of dynamical equation of the present problem, a new coordinate system suitable for analysing spherical shape is required. Cylindrical coordinate system seems a good choice because it provides easier formulation of eddy currents around the surface of sphere. Origin of such system is located at the centre *O* of the sphere with radius vector *r* pointing out towards the surface, located at an angle θ from positive *x*-axis, and azimuthal axis *y* pointing inwards the plane of the figure, as show in Figure 3.

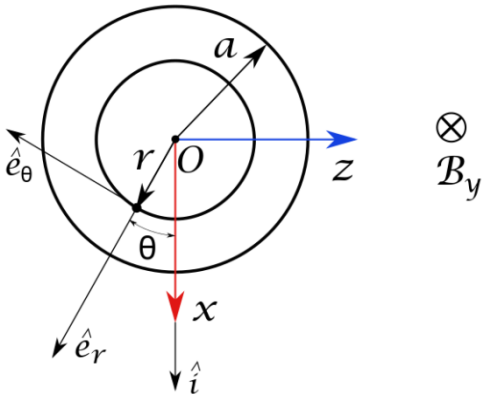

Figure 3 Cylindrical coordinate system $O_{(r,\theta,y)}$.

Taking curl of equation (9) to find the dependence of electric density vector $\vec{j}$ on coordinate axes (x,y,z) it is found that $\partial j/\partial z = 0$.

Boundary condition for a current flowing around the characteristic surface for the cylindrical coordinate system is written as following:

$$y = \pm\sqrt{a^2 - r^2} \tag{11}$$

Moreover, normal unit vector $\hat{n}$ of the characteristic surface points perpendicular to the direction of electric current density vector, thus $\vec{j} \cdot \hat{n} = 0$. Defining a scalar function $F(r, \theta, y)$ representing the surface of the sphere of radius *r* to find the normal vector $\hat{n}$ [10].

$$F(r, \theta, y) = \mp y - \sqrt{a^2 - r^2} \tag{12}$$

Function $F(r, \theta, y)$ values to zero on the surface of the sphere of radius *a*, implying that surface at radius a is of constant value regarding this function. The gradient of $F(r, \theta, y)$ as evaluated in equation (12) is perpendicular to the constant value surface [10].

$$\nabla F = \mp \hat{e}_y - \frac{r}{\sqrt{a^2 - r^2}} \hat{e}_r \tag{12}$$

Equation (12) is normalised to get normal unit vector for the characteristic surface of radius *r* as following:

$$\hat{n} = \mp \sqrt{1 - \left(\frac{r}{a}\right)^2}\, \hat{e}_y - \frac{r}{a} \hat{e}_r \tag{13}$$

Satisfying the condition $\vec{j} \cdot \hat{n} = 0$, equation (13) gives the boundary condition for electric current density.

$$\mp \sqrt{1 - \left(\frac{r}{a}\right)^2}\, j_y - \frac{r}{a} j_r = 0 \tag{14}$$

It is known that $\frac{\partial j}{\partial z} = 0$, thus it can be deduced that *j* is the function of *r* and θ only. Subsequently reducing the equation (14) to positive and negative parts and then adding and subtracting them, it is found that j_r and j_y are zero, leaving j_θ as the only non-zero component. Further referring to the expression (9) it is found that $\frac{\delta j_\theta}{\delta \theta} = 0$, leaving j_θ as the function of *r* alone, $j = j_\theta(r)\hat{e}_\theta$. Transforming equation (9) into cylindrical coordinate system and replacing velocity and magnetic field with expression (8),

$$\vec{j}_\theta(r) = -\sigma \left[\frac{1}{r}\frac{\partial \phi}{\partial \theta} + (-v)\hat{k} \times \left(B_0 + r \sin\theta \frac{\partial B_0}{\partial z}\right)\hat{j}\right]$$

Which can be evaluated to give θ - component of electric density vector,

$$\vec{j}_\theta(r) = -\sigma \left[\frac{1}{r}\frac{\partial \phi}{\partial \theta} - v \sin\theta \left(B_0 + r \sin\theta \frac{\partial B_0}{\partial z}\right)\hat{e}_\theta\right] \tag{15}$$

Integrating the expression (15) from $\theta \to 0\ to\ 2\pi$ and dividing the integration by 2π, the final expression for current density vector for complete sphere is obtained.

$$\vec{j}_\theta(r) = \frac{\sigma r v}{2} \frac{\partial B_0}{\partial z} \hat{e}_\theta \tag{16}$$

Specific Lorentz body force on the spherical element of radius *r* is written as $d\vec{f}_L = \vec{j} \times \vec{B}$ [11]. Replacing $\vec{j}$ with $\vec{j}_\theta(r)$ from equation (16) and $\vec{B}$ with expression (8),

$$d\vec{f}_L = \frac{\sigma r v}{2} \frac{\partial B_0}{\partial z} \left(B_0 + r \sin\theta \frac{\partial B_0}{\partial z}\right) \hat{e}_r \tag{17}$$

Therefore, the net force on the spherical volume element $dV = r dr\, d\theta\, dy$ in *z* - direction is written as [10],

$$dF_L^z = d\vec{f}_L \cdot \hat{k} dV \tag{18}$$

Integrating the equation (18) for the boundary condition defined in expression (11) and $\theta \to 0\ to\ 2\pi$, force on the complete sphere is obtained.

$$F_L^z = \int_0^a \int_{-\sqrt{a^2-r^2}}^{\sqrt{a^2-r^2}} \int_0^{2\pi} \frac{\sigma r v}{2} \frac{\partial B_0}{\partial z} \left(B_0 + r \sin\theta \frac{\partial B_0}{\partial z}\right)(-\sin\theta)\, r d\theta\, dy\, dr \tag{19}$$

Evaluating the integration (19), following expression for total Lorentz force along *z*-axis is obtained:

$$F_L^z = -\frac{2}{15} \pi a^5 \sigma v \left(\frac{\partial B_0}{\partial z}\right)^2 \tag{20}$$

Additionally force on the sphere can be written as $F_L^z = m\frac{dv}{dt} = \frac{4}{3}\pi a^3 \rho \frac{dv}{dt}$, which is equated with expression (20) to give equation for the dynamic motion of sphere through longitudinal magnetic field.

$$\frac{dv}{dt} + \frac{\sigma a^2}{10\rho} v \left(\frac{\partial B_0}{\partial z}\right)^2 = 0 \tag{21}$$

3. Orbital dynamics

For the given system of orbital debris remover along with the debris following assumptions are made before implementing the mathematical model:

- Mass of the debris remover and debris is relatively small compared to the mass of the Earth, so only the gravitational force due to Earth is prevalent in the system.
- The system is studied under the aspects of planar motion.
- Debris is located in a circular orbit with zero inclination, therefore its eccentricity is zero.
- Distance between debris remover and the debris is very small in comparison their respective altitudes.
- Debris remover (also named collector) moves with constant acceleration in along-track direction.
- Thrust force *P* acting on the collector is very small, of the order milli Newton.
- The debris is electrically conductive and has magnetic susceptibility (paramagnetic/ diamagnetic).

For the current problem it is vital that the information about the motion of debris relative to the debris remover is known, so that the removing process can be implemented correctly. For such a task it is necessary to switch to a relative reference system, in which the relative trajectory of the debris can be computed. For such a case, Hill's reference frame is a good choice. The idea is illustrated in Figure 4.

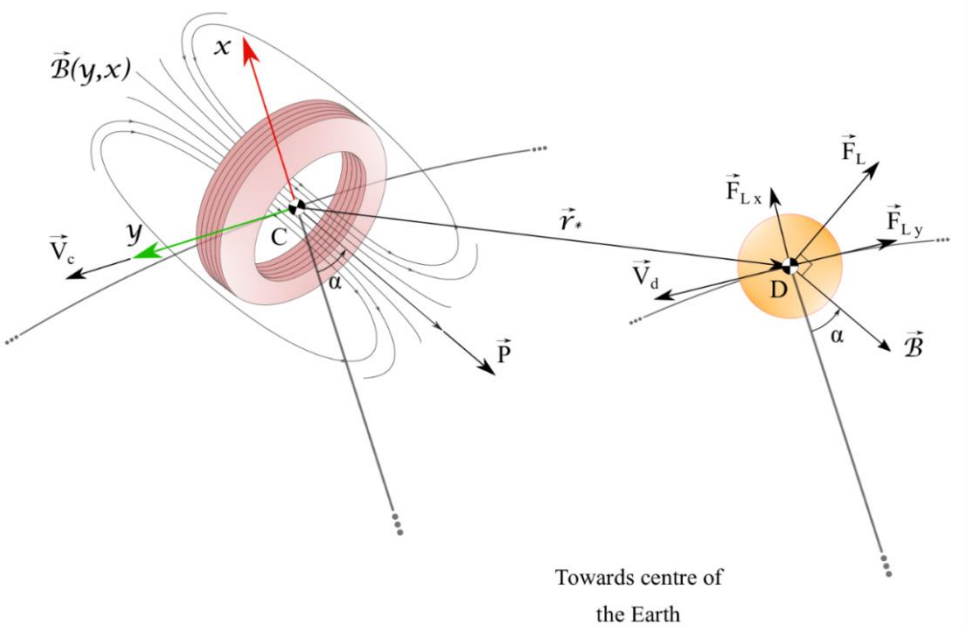

Figure 4. Illustration of relative motion of the debris in a constantly accelerating Hill's reference frame.

Let us consider the Hill's reference system *Cxy* located at the center of mass of the debris remover, with *x*-axis pointing toward the local vertical and y-axis tangent to the trajectory of the debris remover. The location of an object relative to point *C* can be given in the form of a position vector $\vec{r}_* = [x, y]^T$ pointing to the center of mass of that particular object. Additionally, the debris remover is constantly accelerating due to the action of thrust force *P* pointing in the along-track direction. Therefore, the trajectory of Hill's reference frame is a spiral, with time-varying orbital speed.

The rate of change of orbital speed is computed using following expression:

$$\dot{n} \approx \frac{P}{M r_{cd}} \tag{23}$$

Where M is the total mass of the system, $\hat{r}_{cd}$ is the unit vector pointing in the direction of position vector of center of mass of the system with respect to the center of the Earth. Recalling that the thrust force $\vec{P}$ is very small in magnitude, and considering the total mass of the system is $3000\,kg$, rate of change of orbital speed during transfer from geostationary orbit – $35{,}786\,km$ to the graveyard orbit is computed as following:

$$\dot{n} = \frac{10 \cdot 10^{-3}}{3000 \cdot (35786 + 6378) \cdot 10^{3}} = 7.9 \cdot 10^{-14} \tag{24}$$

It is evident that for the considered set of parameters time-rate of change of orbital speed is very small. Thus, the angular rate $\dot{n}$ will be considered as a constant for subsequent modelling.

Equation of planar relative motion of the debris in previously implemented Hill's reference frame can be adequately written in the form of linear Clohessy-Wiltshire equations [12, p. 279].

$$\begin{cases} \ddot{x} = 3n^2 x + 2n\dot{y} + a_x \\ \ddot{y} = -2n\dot{x} + a_y \end{cases} \tag{25}$$

Where a_x and a_y are projections of relative acceleration along *x* and *y* axes, respectively. And n is the orbital rate of the system which is written in the following form:

$$n = \sqrt{\frac{\mu_E}{r_s^3}} \tag{26}$$

Here μ_E is the gravitational parameter of the Earth and r_s is the average orbital radius of the system. Recalling that the time-rate of change of *n* is very small, hence it can be written out as a constant. Moreover, the projections of acceleration include terms for external thrust $\vec{P}$ on the collector and Lorentz force due to the collector, debris and the Earth:

$$\vec{a} = \{\vec{a}_{Lc} + \vec{a}_{Ld}\} - \frac{\vec{P}}{m_1} \tag{27}$$

Where a_{Lc} is the acceleration due to Lorentz force on collector due to induced magnetic field of the debris in motion.

$$a_{Lc} = -\frac{\sigma_c R_c^2}{8\rho_c} V_c (B'_{i\,d})^2 \tag{28}$$

While a_{Ld} is the acceleration due to Lorentz force on the debris due to magnetic field of the collector in motion, defined in section 2.2 equation (21).

$$a_{Ld} = -\frac{\sigma_d R_d^2}{10\rho_d} V_d (B'_c)^2 \tag{29}$$

Here σ, R, V and ρ is conductivity, radius, velocity and density of the respective objects – Collector and Debris. $B'_{i\,d}$ and B'_c is the derivative of the induced magnetic field of debris and the inducing magnetic field of collector with respect to local coordinates, respectively.

Mathematical analysis of relative motion of coil-debris system demands information regarding separation distance and angular position of the debris relative to the centre of the coil. This information can be conveniently extracted during the numerical simulation of the system if transformed into polar coordinates from the current Cartesian coordinates. The transformation can be carried out using following substitutions:

$$y = d\cos\alpha\,, \quad x = d\sin\alpha \tag{30}$$

After substituting the variables x and y in equation (25) using expressions (32), the Clohessy-Wiltshire equations are re-written in polar coordinates as,

$$\begin{cases} \ddot{\alpha} = 2(n - \dot{\alpha})\dfrac{\dot{d}}{d} + \dfrac{3n^2}{2}\sin 2\alpha + \left\{a_{Lc}^{(\alpha)} - a_{Ld}^{(\alpha)}\right\} + \dfrac{a_P}{d}\sin\alpha \\ \ddot{d} = (3n^2\sin^2\alpha - 2n\dot{\alpha} + \dot{\alpha}^2)d + \left\{a_{Lc}^{(d)} - a_{Ld}^{(d)}\right\} - a_P\cos\alpha \end{cases} \tag{31}$$

Where $\left\{a_{Lc}^{(\alpha)} - a_{Ld}^{(\alpha)}\right\}$ and $\left\{a_{Lc}^{(d)} - a_{Ld}^{(d)}\right\}$ are components of Lorentz force acting on the coil and debris along angular and radial directions, respectively. a_P is the acceleration due to constant thrust acting on the collector.

The magnetic vector potential of the coil is defined by expression (32), which is accurate for coil with N number of turns [13, p. 182].

$$A_\phi(d,\theta) = \frac{\mu_0}{4} n_c I \frac{R^2 L\, d \sin\theta}{(d^2 + R_c^2)^{3/2}} \left(1 + \frac{15\, R_c^2\, d^2 \sin^2\theta}{8(d^2 + R_c^2)^2}\right) \tag{32}$$

Here, $n_c = {}^{N}/_{L}$ is the turn density of the coil, while I is the input current of the coil. Magnetic field strength B can be evaluated from expression (32) as following:

$$B_d = \frac{1}{d \sin\theta} \frac{\partial}{\partial\theta}\left(A_\phi \sin\theta\right), \quad B_\theta = -\frac{1}{d} \frac{\partial}{\partial d}\left(d A_\phi\right) \tag{33}$$

It should be noted that above magnetic field distribution is ideal for three regions around the coil: far from the coil ($R_c \ll d$), near the center of the coil ($R_c \gg d$), and near the axis of the coil ($\theta \ll 1$).

4. Numerical simulation

4.1 System parameters

Let us consider the system parameters as mentioned in Simulation results

Change in relative distance d of spherical debris with respect to the collector with different values of input current during transfer maneuver is shown in Figure 5 (a) and (b). Change in polar coordinate angle α relative to the collector and semi-major axis of the debris is shown in Figure 5 (c) and (d), respectively.

Table 1. Pertaining to the fact that the orbital rate *n* is considered constant, the set of equations (31) are therefore linear and time-invariant. Additionally, identifying the limitations of the classical Clohessy-Wiltshire equations that they are the approximations of two-body dynamics and valid only for small deviation from the reference state [12]. Because, the set of equations (31) are linear, it is possible to numerically solve them with a good accuracy around local vertical.

The system is numerically solved for different values of the current *I* ranging from 0 A to 20 A. Time period for evaluation is calculated by analyzing the transfer time of the system for given orbital parameters using following formula [12, p. 310]:

$$t_{transfer} = c \frac{(m_1 + m_2)}{P}\left[1 - exp\left(\frac{-\Delta v}{c}\right)\right] \tag{34}$$

Where v_e is the effective jet exhaust velocity of the ion thruster engine. Δv is the difference between orbital velocity of the initial (geostationary) orbit, h and the target (graveyard) orbit, $(h + \Delta h)$.

Replacing the parameters in formula (34) with their respective values gives transfer time equals to $25.2787\ days$, during which the location of debris (sphere shaped) with respect to the collector is computed for each step. It is further noted that magnetic field strength of Earth at geostationary orbit is in the order of micro Tesla, which is significantly lower than magnetic field strength of the coil [7]. Thus, contribution of magnetic field of Earth has not been considered with insignificant loss of precision related to relative position of the debris.

Change in semi-major axis of the system during transfer maneuver is computed using following equation [12, p. 309]:

$$a(t) = \frac{\mu}{\left[v_0 - c \ln\left(\frac{\tau}{\tau - t}\right)\right]^2} \tag{35}$$

Where time constant $\tau = m_1/\dot{m} = m_1 c/P$. And, initial orbital velocity $v_0 = \sqrt{\mu/(R_E + h)}$.

Initial conditions for the current system are as mentioned below:

$$\begin{aligned} d(0) &= 5\ m, & \dot{d}(0) &= 0\ m/s \\ \theta(0) &= 0.1\ rad, & \dot{\theta}(0) &= 0\ rad/s \end{aligned} \tag{36}$$

4.2 Simulation results

Change in relative distance d of spherical debris with respect to the collector with different values of input current during transfer maneuver is shown in Figure 5 (a) and (b). Change in polar coordinate angle α relative to the collector and semi-major axis of the debris is shown in Figure 5 (c) and (d), respectively.

Table 1. System parameters.

Parameter, SI unit	Symbol	Value
Inner radius of the coil, m	R_c	1.5
Radius of the sphere (debris), m	R_d	0.1
Axial length of the coil, m	L	0.5
Mass of the collector, kg	m_1	3,000
Number of turns, N	N	10,000
Density of the collector, kg/m^3	ρ_c	$2 \cdot 10^3$
Density of the sphere, kg/m^3	ρ_d	$1.5 \cdot 10^3$
Electrical conductivity of the collector, S/m	σ_c	10^4
Electrical conductivity of the sphere, S/m	σ_d	$4 \cdot 10^6$
Altitude, km	h	35,786
Desired change in altitude, km	Δh	200
Permeability constant, T · m/A	μ	$4\pi \cdot 10^{-7}$
Gravitational parameter of the Earth, m^3/s^2	μ_E	$3.986044 \cdot 10^{14}$
Radius of the Earth, km	R_E	6378
Thrust force, mN	P	10
Effective jet exhaust velocity, km/s	c	20

It is apparent from plot (b) that during the application of input current of value $15\,A$ and $20\,A$ debris is moving towards the center of the coil near the axis with very small relative velocity. On a different case, debris quickly moves towards and then away from the center during the application of input current of value $5\,A$ and $10\,A$. This behavior can be understood by analyzing plot (c) for polar coordinate α, where it can be observed that the angle α changes from $0°$ to $360°$ relatively faster during the application of input current equal to $5\,A$ and $10\,A$, than during the application of input current equal to $15\,A$ and $20\,A$. The cause for this phenomenon is the peak value of magnetic field strength at the center of the coil, which is directly proportional to the magnitude of input current.

Evidently, greater input current generates strong and axially concentrated magnetic field distribution [13]. Higher concentration of magnetic field in a region tends to generate stronger Lorentz force on a conductive object moving through this region. Additionally, the Lorentz force acts in the direction opposite to the direction of motion. Therefore, higher magnitude of Lorentz force imparts greater deceleration to the object in motion. Similarly, for the case of collector-debris in orbit, the conductive debris object is decelerated such, that it appears to be "captured" by the collector. This can be validated from Figure 5 (a) – (c) by examining plots of variables d and α when $I = 15\,A$ and $I = 20\,A$. Where it can be seen that variable d varies gradually from $5\,m$ to $0.15\,m$ in the span of 25 days, while angle α varies almost linearly from $0°$ to $90°$ when $I = 20\,A$. For the case when $I = 15\,A$, the object comes close to the center of the collector by $0.15\,m$, and subsequently there is a rapid change in the angle α at $t = 15\,days$ which denotes the departure of the object from the coil in the opposite direction of the motion of collector. This is indeed the case when $I = 20\,A$, for which the departure happens latter the transfer time, therefore the debris is delivered to the graveyard orbit before it departs away from the collector. This is graphically presented in Figure 5 (d), wherein it can be observed that semi-major axis a of the debris changes virtually linearly during the span of transfer time of 25 days when $I = 15\,A$ and $I = 20\,A$. For rest of the cases the debris is observed to be departing away from the collector before the end of transfer time.

5. Conclusion

Numerical simulation for the proposed system showed that different magnitudes of input currents have particular set of consequences. With higher input currents ($I = 15\,A, 20A$) are able to effectively change the semi-major axis of the debris. The proposed technique has potential use for removing conductive space debris such as discarded fuel tanks, higher stages and combustion chambers which are generally made from copper alloys.

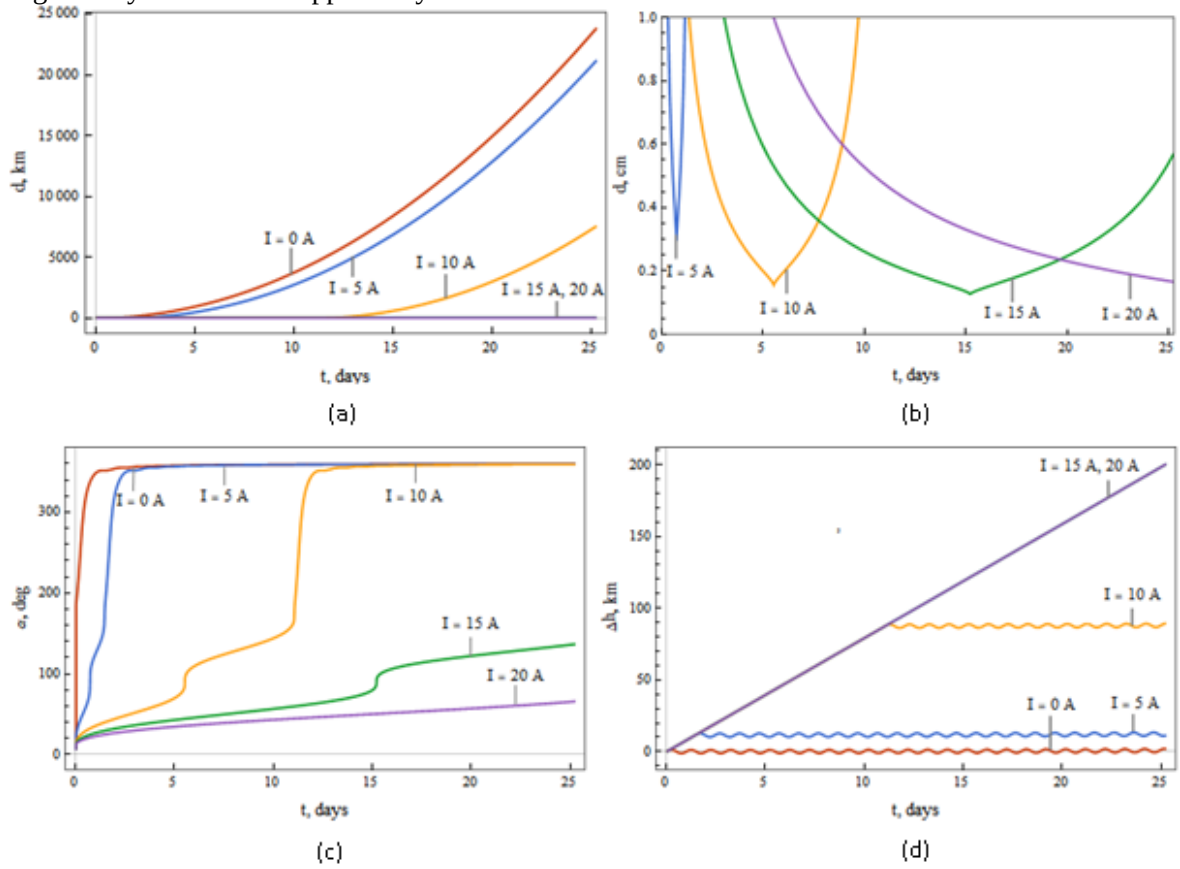

Figure 5. Time history of (a) polar coordinate d – Full-scale view, (b) polar coordinate d – Magnified view of the centre of the coil, (c) polar coordinate α; (d) Change in semi-major axis Δh of the debris during the transfer manoeuvre.

Although the study was conducted for an electrically conductive object, the method is not applicable for objects with low conductivity. Additionally, effects of plasma interaction and gravitational perturbations of heavenly bodies has not been studied, yet. A motion control technique for orbit correction is being developed, which is a topic for a separate research paper. An in-depth study is required to be undertaken to analyze the electromagnetic interaction with differently shaped objects at different altitudes.

6. Acknowledgments

This study was supported by the Russian Foundation for Basic Research (RFBR 18-01-00215-A).

7. References

[1] ARES | Orbital Debris Program Office [Electronic resource]. – Access mode: https://orbitaldebris.jsc.nasa.gov/ (16.10.2019).

[2] Hortstmann, A. Survey of the Current Activities in the Field of Modeling the Space Debris Environment at TU Braunschweig / A. Hortstmann // Aerospace. – 2018. – Vol. 5(2). – P. 37. DOI: 10.3390/aerospace5020037.

[3] Mark, C.P. Review of Active Space Debris Removal Methods / C.P. Mark, S. Kamath // Space Policy. – 2019. – Vol. 47. – P. 194-206. DOI: 10.1016/j.spacepol.2018.12.005.
[4] Castronuovo, M.M. Active space debris removal – A preliminary mission analysis and design / M.M. Castronuovo // Acta Astronautica. – 2011. – Vol. 69(9). – P. 848-859. DOI: 10.1016/j.actaastro.2011.04.017.
[5] Aslanov, V.S. Debris removal in GEO by heavy orbital collector / V.S. Aslanov // Acta Astronautica. – 2019. – Vol. 164. – P. 184-191. DOI: 10.1016/j.actaastro.2019.07.021.
[6] Aslanov, V.S. Gravitational Trap for Space Debris in Geosynchronous Orbit / V.S. Aslanov // Journal of Spacecraft and Rockets. – 2019. – Vol. 56(4). – P. 1277-1281. DOI: 10.2514/1.A34384.
[7] Gómez, N.O. Earth's gravity gradient and eddy currents effects on the rotational dynamics of space debris objects: Envisat case study / N.O. Gómez, S.J.I. Walker // Advances in Space Research. – 2015. – Vol. 56(3). – P. 494-508. DOI: 10.1016/j.asr.2014.12.031.
[8] Purcell, E.M. Electricity and Magnetism / E.M. Purcell – Cambridge, 2013. – 200 p.
[9] Griffiths, D.J. Introduction to electrodynamics / D.J. Griffiths – Boston: Pearson, 2013.
[10] Walker, J. Drag force on a conductive spherical drop in a nonuniform magnetic field / J. Walker, W.M. Wells // ORNL/TM-6976. – 1979. – P. 5872573.
[11] Landau, L.D. Electrodynamics of Continuous Media / L.D. Landau, E.M. Lifshitz // Course of Theoretical Physics. – 1984. – Vol. 8. – P. 429.
[12] Kluever, C.A. Space Flight Dynamics // Aerospace Series – Wiley.
[13] Jackson, J.D. Classical Electrodynamics – Wiley.